Available online at www.eccomasproceedia.org
Eccomas Proceedia UNCECOMP (2017) 269-278

ECCOMAS
Proceedia

UNCECOMP 2017
2nd ECCOMAS Thematic Conference on
Uncertainty Quantification in Computational Sciences and Engineering
M. Papadrakakis, V. Papadopoulos, G. Stefanou (eds.)
Rhodes Island, Greece, 15–17 June 2017

IDENTIFICATION AND QUANTIFICATION OF MULTIVARIATE POSSIBILISTIC MANUFACTURING UNCERTAINTY IN DYNAMIC NUMERICAL MODELS

M. Faes [1], **D. Vandepitte** [2], **D. Moens** [1]

[1]KU Leuven - Department of Mechanical Engineering
Jan De Nayerlaan 5, B-2860 St.-Katelijne-Waver
e-mail: matthias.faes,david.moens@kuleuven.be
[2] KU Leuven, Department of Mechanical Engineering,
Celestijnenlaan 300, B-3001, Leuven, Belgium

Keywords: Uncertainty Quantification, Multivariate interval uncertainty

Abstract. *The objective of this work to validate a novel methodology for the identification and quantification of possiblistic multivariate uncertainty that has been presented by the authors in previous work. The method is based on the convex hull concept for both the representation of uncertainty in the result of an interval finite element computation, as for the variability that was measured on the real-life structure. Identification of the parameteric multivariate interval uncertainty is performed by minimisation of a metric describing the discrepancy between these convex hulls. This method has been proven to be able do deliver an accurate identification of multivariate possibilistic uncertainty, which is also robust against certain measurement set metrics, however only on small-scale academic examples. This paper therefore first introduces a generic method for the reduction of the dimensionality of the identification at hand, and shows a validation of the method on a high-dimensional, complicated numerical model. Specifically, a test structure containing uncertainty in the stiffness of several bolted connections, introduced during the assembly of the structure, will be considered. The uncertainty in the stiffness of these connections is identified by using the presented method.*

Peer-review under responsibility of the organizing committee of UNCECOMP 2017.
doi: 10.7712/120217.5368.16713

1 INTRODUCTION

In the context of incorporating uncertainty on model parameters into the numerical design models that are increasingly being used in industrial design processes, the interval method has been shown to give an accurate prediction of the occuring uncertainty in the model responses, based on limited data sets. Following this technique, the non-determinism is depicted as an interval on the model parameters thus propagated through the numerical model, thus eliminating the need for the identification of a full probabilistic data description, as needed for the probabilistic counterparts, which may be very cumbersome. Moreover, less expensive numerical procedures are necessary for the description of the variability [4, 11, 8], which makes these techniques highly suitable for early design stages.

However, in order to obtain a realistic assessment of the non-determinism in the responses of the model under consideration, an accurate estimation of the interval uncertainty at the input side of the model is pre-emptive. The authors proposed in this context a generic methodology for the identification of multivariate interval uncertainty [3, 2], based on the computation of the convex hulls over the computed realisations of the input non-determinism and the set of repeated measurement data. However the promising results obtained on simple academic cases, no validation of the method was performed on a model having a realistic amount of degrees of freedom. In order to apply the methodology on high-dimensional datasets, the dimensionality has to be reduced due to the exponential complexity of the computation of the convex hulls. This paper therefore introduces a generic reduction scheme. The method, including the identification procedure, is illustrated using the AIRMOD test structure (see e.g., [6, 5, 7, 13]) in order to show the performance of the method in a realistic model in conjunction with a high-dimensional interval uncertainty associated with the parameters of the model.

2 MULTIVARIATE INTERVAL IDENTIFICATION

By definition, an interval parameter x is indicated using apex I: x^I. Vectors are expressed as lower-case boldface characters $\mathbf{x}$, whereas matrices are expressed as upper-case boldface characters $\mathbf{X}$. For the remainder of the text, interval parameters are either represented using the bounds of the interval $x^I = [\underline{x}; \overline{x}]$ or the centre point $\hat{x} = \frac{\underline{x}+\overline{x}}{2}$ and interval radius $r_x = \frac{\overline{x}-\underline{x}}{2}$.

2.1 The interval finite element method

2.2 Interval finite elements

The interval field FE method comes down to finding the solution set $\tilde{\mathbf{y}}$, when the model parameter uncertainty is depicted as an interval field $\boldsymbol{\gamma}_F^I(\mathbf{r}) \in \mathbb{IR}^k$ over the geometrical model domain Ω, with $\mathbb{IR}^k$ the k-dimensional space of interval scalars and $\mathbf{r} \in \Omega \subset \mathbb{R}^t$. $\tilde{\mathbf{y}}$ usually spans a multidimensional non-convex region in $\mathbb{R}^d$, and is therefore commonly approximated by an uncertain realization set $\tilde{\mathbf{y}}_s$, which is obtained by propagating q deterministic realizations $\mathbf{y}_{sj}$ of the interval field $\boldsymbol{\gamma}_F^I(\mathbf{r})$:

$$\tilde{\mathbf{y}}_s = \left\{ \mathbf{y}_{sj} \mid \mathbf{y}_{sj} = f(\boldsymbol{\gamma}_{F,j}(\mathbf{r})); \boldsymbol{\gamma}_{F,j}(\mathbf{r}) \in \boldsymbol{\gamma}_F^I(\mathbf{r}) \right\} \tag{1}$$

Herein, $\mathbf{y}_{sj}$ is a vector containing the d output responses of the deterministic solution of the propagation of the j^{th} input uncertainty realization, with $j \in [1, q]$:

$$\mathbf{y}_{sj} = [y_{s1},\ y_{s2},\ ..,\ y_{sd}] \tag{2}$$

These q deterministic propagations should represent the solution set $\tilde{\mathbf{y}}$ as close as possible. In the case of strict monotonicity of $f()$, also the transformation method [8] can be used.

2.3 Multivariate interval identification

This section explains the novel methodology for the identification and quantification of multivariate interval uncertainty, as presented by the authors in [2, 3]. This methodology is based on the comparison of a set of repeated real-live measurements $\tilde{\mathbf{y}}_m$, performed on the physical component under consideration, with the result of the interval computation $\tilde{\mathbf{y}}_s$. For the comparison, a convex polytope is constructed around $\tilde{\mathbf{y}}_m$ and $\tilde{\mathbf{y}}_s$. Specifically, the convex hulls of $\tilde{\mathbf{y}}_m$ and $\tilde{\mathbf{y}}_s$, respectively $\mathcal{C}_m$ and $\mathcal{C}_s$, as well as the corresponding d-dimensional volumes V_m and V_s, are hereto computed. All convex hull computations are performed using the QHULL library, which makes use of the Quickhull algorithm [1]. Identification of $\boldsymbol{\alpha}^I$ is performed by minimising a cost function $\delta(\boldsymbol{\alpha}^I)$, which described the discrepancy between $\tilde{\mathbf{y}}_s$ and $\tilde{\mathbf{y}}_m$:

$$\delta(\boldsymbol{\alpha}^I) = \left(\Delta V_m^2 + \Delta V_o^2 + \Delta c^2\right) \tag{3}$$

with:

$$\Delta V_m = 1 - \frac{V_s(\boldsymbol{\alpha}^I)}{V_m} \tag{4a}$$

$$\Delta V_o = 1 - \frac{V_o(\boldsymbol{\alpha}^I)}{V_m} \tag{4b}$$

$$\Delta c = \left\|\mathbf{c}_m - \mathbf{c}_s(\boldsymbol{\alpha}^I)\right\|_2 \tag{4c}$$

with $\mathbf{c}_m$ and $\mathbf{c}_s$ the geometrical centres of mass of respectively $\tilde{\mathbf{y}}_m$ and $\tilde{\mathbf{y}}_s$. V_o is the multidimensional volume of the overlap $\tilde{\mathbf{y}}_o$ between $\tilde{\mathbf{y}}_m$ and $\tilde{\mathbf{y}}_s$. The interval vector $\boldsymbol{\alpha}^{I,*}$, used for the construction of $\boldsymbol{\gamma}_F^I(\mathbf{r})$, is finally determined as :

$$\boldsymbol{\alpha}^{I,*} = \text{argmin}\left(\delta(\boldsymbol{\alpha}^I)\right) \tag{5}$$

2.4 Response set dimensionality reduction

The numerical computation of the convex hull and the corresponding multi-dimensional volume is done using the QHULL library, which uses the "Quickhull" algorithm, as developed by **Barber et al.** [1]. The time complexity, of the *Quickhull* computation of a convex hull is in a worst case scenario:

$$\mathcal{O}(\lfloor v_c^{\frac{d}{2}} \rfloor / \lfloor \frac{d}{2} \rfloor !) \tag{6}$$

with v_c the number of vertices of $\mathcal{C}_s$[1]. Therefore, care should be taken when computing convex hulls over large response vectors in $\mathbb{R}^d$.

In order to prevent the computation of the convex hulls in general d dimensions, the measurement data set and uncertain realisation set are projected onto a d_r-dimensional orthogonal basis, with $d_r << d$. In a first step, an orthogonal basis $\mathcal{B}$ is constructed in $\mathbb{R}^{d_r}$, which is defined as:

$$\mathcal{B} = \{\boldsymbol{\phi}_{m,d-d_r}, \boldsymbol{\phi}_{m,d-d_r+1}, ...\boldsymbol{\phi}_{m,d}\} \tag{7}$$

with d_r chosen as such that all non-zero dimensions are included in $\mathcal{B}$, and $\boldsymbol{\phi}_m$ the eigenvectors corresponding to the d_r largest eigenvalues of the covariance structure of the measurement data set $\tilde{\mathbf{y}}_m$. Subsequently, all $\frac{d_r!}{d_r^+!(d_r-d_r^+)!}$ d_r^+-dimensional projections from this $\mathbb{R}^{d_r}$-dimensional are constructed, and they are gathered in a set $\mathcal{B}^+$.

For the actual reduction, the realisations $\mathbf{y}_{sj} \in \tilde{\mathbf{y}}_s$ are first normalised to a normalised interval $\mathbf{y}_{sj}^n$, having following properties:

$$\hat{\mathbf{y}}_{sj}^n = 0 \tag{8}$$

$$r_{\mathbf{y}_{sj}^n} = 1 \tag{9}$$

These $\mathbf{y}_{sj}^n$ are subsequently concatenated into a matrix $\tilde{\mathbf{Y}}_s^n \in \mathbb{R}^{d \times q}$, which is defined as:

$$\tilde{\mathbf{Y}}_s^n = [\mathbf{y}_{s1}^n, \mathbf{y}_{s2}^n, ..., \mathbf{y}_{sq}^n] \tag{10}$$

with $\mathbf{y}_{sj}^n$, $j = 1..., q$ the q realisations of $\tilde{\mathbf{y}}_s$, and are then projected onto the i^{th} projection $\mathcal{B}_i^+$ of the orthogonal basis $\mathcal{B}$ such that:

$$\tilde{\mathbf{Y}}_s^{n,r} = \tilde{\mathbf{Y}}_s^T \mathcal{B}_i^+ = [\hat{\mathbf{y}}_{s1}^{n,r}, \hat{\mathbf{y}}_{s2}^{n,r}, ..., \hat{\mathbf{y}}_{sq}^{n,r}] \tag{11}$$

The q realisations $\hat{\mathbf{y}}_{sj}^{n,r} \in \mathbb{R}^{d_r}$, $j = 1..., q$ of the projected, and thus lower-dimensional, uncertain realisation matrix $\tilde{\mathbf{Y}}_s^{n,r}$ are then used to construct the reduced uncertain realisation set $\tilde{\mathbf{y}}_s^r$. The convex hulls $\mathcal{C}_m$ and $\mathcal{C}_s$ are also computed in the d_r^+ dimensional projections of this d_r-dimensional vector space. Incorporating this in the optimisation problem, presented in eq. (5), this yields:

$$\delta(\boldsymbol{\alpha}^I) = \sum_{i=1}^{\frac{d_r!}{d_r^+!(d_r-d_r^+)!}} \left(\Delta V_m^2(\mathcal{B}_i^+) + \Delta V_o^2(\mathcal{B}_i^+) + \Delta c^2(\mathcal{B}_i^+)\right) \tag{12}$$

with:

$$\Delta V_m = 1 - \frac{V_s(\boldsymbol{\alpha}^I, \mathcal{B}_i^+)}{V_m(\mathcal{B}_i^+)} \tag{13a}$$

$$\Delta V_o = 1 - \frac{V_o(\boldsymbol{\alpha}^I, \mathcal{B}_i^+)}{V_m(\mathcal{B}_i^+)} \tag{13b}$$

$$\Delta c = \left\| \mathbf{c}_m - \mathbf{c}_s(\boldsymbol{\alpha}^I) \right\|_2 \tag{13c}$$

and where $(\mathcal{B}_i^+)$ is used to indicate that the respective multidimensional volumes are computed using the i^{th} projection of the d_r dimensional orthogonal basis. The total error is computed as the sum of squared errors over all considered projections.

3 CASE STUDY

3.1 AIRMOD model

The DLR AIRMOD structure is used in this paper to demonstrate the application of the proposed uncertain set reduction method and the corresponding indentification procedure. First, a measurement data set is generated by forward propagation of well-defined intervals that are

defined on model parameters. This high dimensional data set is subsequently reduced by projecting it on a lower-dimensional basis. The identification of the interval uncertainty, based on the method presented in [3, 2], is then performed using well-defined projections of the measurement data set in this lower-dimensional basis.

Table 1: Non-rigid eigenmodes and eigenfrequencies of the deterministic model

	Description	f	n_o	Description	f
1	2^{nd} wing bend	$5.50\ Hz$	14	7^{th} wing bend	$145.91\ Hz$
2	3^{rd} wing bend	$15.11\ Hz$	15	2^{nd} HTP bend	$206.73\ Hz$
3	1^{st} ant-sym. wing tors	$31.31\ Hz$	16	1^{st} HTP fre-aft bend	$225.73\ Hz$
4	1^{st} sym. wing tors	$33.62\ Hz$	17	1^{st} wing bend right	$261.53\ Hz$
5	1^{st} VTP bend	$35.39\ Hz$	18	1^{st} wing bend left	$262.64\ Hz$
6	4^{th} wing bend	$44.66\ Hz$	19	3^{rd} wing fre-aft bend	$278.71\ Hz$
7	1^{st} wing fre-aft bend	$47.21\ Hz$	20	1^{st} winglet bend left	$320.15\ Hz$
8	2^{nd} wing fre-aft bend	$52.91\ Hz$	21	1^{st} winglet bend right	$321.64\ Hz$
9	5^{th} wing bend	$60.59\ Hz$	22	3^{rd} fuselat bend	$324.12\ Hz$
10	1^{st} VTP tors	$67.69\ Hz$	23	2^{nd} sym. wing tors	$336.31\ Hz$
11	2^{nd} fuse lat bend	$102.59\ Hz$	24	2^{nd} ant-sym. wing tors	$341.15\ Hz$
12	2^{nd} VTP bend	$128.62\ Hz$	25	4^{th} wing fre-aft bend	$343.55\ Hz$
13	6^{th} wing bend	$132.08\ Hz$	26	$2nd$ fuse vert bend	$359.54\ Hz$

The DLR AIRMOD structure is a scaled replica of the GARTEUR SM-AG19 benchmark. The physical AIRMOD structure is constructed from six aluminum beams that are connected by five bolted joints and weighs approximatly 40 kg to represent the fuselage, wings, winglets, vertical tail plate (VTP) and horizontal tail plate (HTP). It has a wing span of 2.0 m, the fuselage length is 1.5 m and the height is 0.46 m. The complete FE model, constructed in NX Nastran, consists of 1440 CHEXA, 6 CPENTA and 561 CELAS1, 55 CMASS1, 18 CONM2 and 3 CROD elements, and is constructed after e.g., [5, 7, 13, 6]. This model is shown in figure **??**

A set of 14 parameters including support and joint stiffness values, as well as mass parameters are selected for the benchmarking. These parameters, together with their deterministic values are shown in table 2. Identification of the corresponding interval uncertainty is hence an identification problem in 28 dimensions. This model provides a challenge for the identification procedure due to high dimensionality of the problem, as well as the combination of symmetric/anti-symmetric mode combinations, as well as closely spaced eigenfrequencies. Table 1 lists the non-rigid eigenfrequencies that are obtained by solving the deterministic model. As may be noted, closely spaced eigenfrequencies are located around $30\ Hz$ and $320\ Hz$. From this set, the 1^{st}, 2^{nd},4^{th},$8^{th} - 14^{th}$ and 26^{th} eigenfrequency are selected for the identification.

Measurement data are generated by sampling a predefined set of intervals on the input parameters. The intervals that were used to construct the set of measurement data is shown in table 3 (indicated as α^*). Specifically, 85 samples are taken out of a uniform distribution between these interval boundaries. Special care is taken to track mode shifts between the different realisations. This is done by MAC-based mode correlation.

3.2 Surrogate modelling

The interval model is solved using the Transformation Method, leading to $2^{14} = 16384$ deterministic model evaluations. Since each deterministic model evaluation takes approx. 10

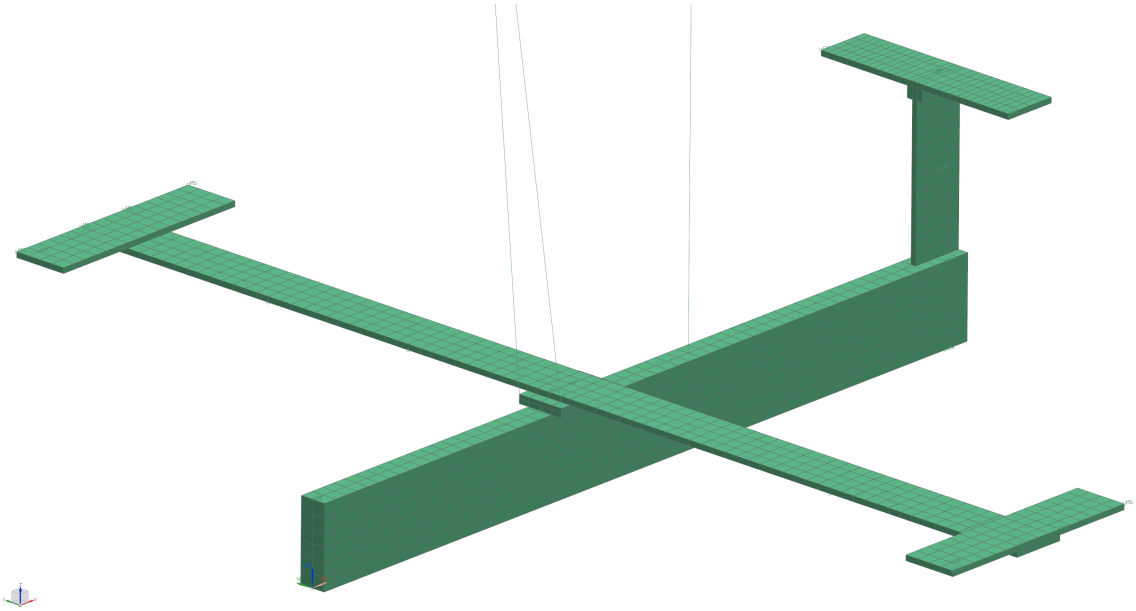

Figure 1: Illustration of the Finite Element model of the AIRMOD test structure

Table 2: Parameters that are used in the identification

	Type	Description	Location	Orientation	Det. value
γ_1	Stiff.	Sensor cable	VTP/HTP joint	y	$1.30 \cdot 10^{02}\ N/m$
γ_2	Stiff.	Sensor cable	WING/FUSELAGE joint	y	$7.00 \cdot 10^{01}\ N/m$
γ_3	Stiff.	Joint Stiff.	VTP/HTP joint	x, y	$1.00 \cdot 10^{07}\ N/m$
γ_4	Stiff.	Joint Stiff.	VTP/HTP joint	z	$1.00 \cdot 10^{09}\ N/m$
γ_5	Mass	Sensor cables	VTP/HTP joint	/	$2.00 \cdot 10^{-01}\ kg$
γ_6	Mass	Screws and glue	Wingtips	/	$1.86 \cdot 10^{-01}\ kg$
γ_7	Mass	Sensor cables	Wingtips	/	$1.50 \cdot 10^{-02}\ kg$
γ_8	Mass	Sensor cables	Outer wing	/	$1.50 \cdot 10^{-02}\ kg$
γ_9	Mass	Sensor cables	Inner wing	/	$1.50 \cdot 10^{-02}\ kg$
γ_{10}	Stiff.	Joint Stiff.	WING/FUSELAGE joint	x	$2.00 \cdot 10^{07}\ N/m$
γ_{11}	Stiff.	Joint Stiff.	WING/FUSELAGE joint	y	$2.00 \cdot 10^{07}\ N/m$
γ_{12}	Stiff.	Joint Stiff.	WING/FUSELAGE joint	z	$7.00 \cdot 10^{06}\ N/m$
γ_{13}	Stiff.	Joint Stiff.	VTP/FUSELAGE	x	$5.00 \cdot 10^{07}\ N/m$
γ_{14}	Stiff.	Joint Stiff.	VTP/FUSELAGE	y	$1.00 \cdot 10^{07}\ N/m$

seconds of wall-clock time on a Intel Xeon E5-2695 @2.30 GHz, evaluating this interval model would take prohibitively long. Therefore, in order to reduce the computational cost, an Artificial Neural Network (ANN) approach is followed. Hereto, a (14:16:14:1) neural network is trained for each individual eigenfrequency based on a dataset containing 10000 Monte Carlo samples drawn from a uniform distribution between 0.1 and 10 times the deterministic values of the model parameters. The size of the network is selected in correspondence with recent work of Patelli et al. [13]. Overtraining is prevented by using Bayesian regularisation for the training of the network [10]. One call to the ANN model (compiled in C++) takes about $0.55s$, when all 16384 deterministic realisation are progagated through in a vectorised fashion (i.e. simultatneouly).

Figure 2 plots 100 randomly drawn samples (which are not included in the training set) from the model against the prediction of the ANN for a selection of eigenfrequencies for the 1^{st}, 2^{nd}, 4^{th}, 6^{th}, 7^{th} and 8^{th} eigenfrequency. As can be noted, a highly accurate prediction of the actual FE model response is obtained by the ANN model.

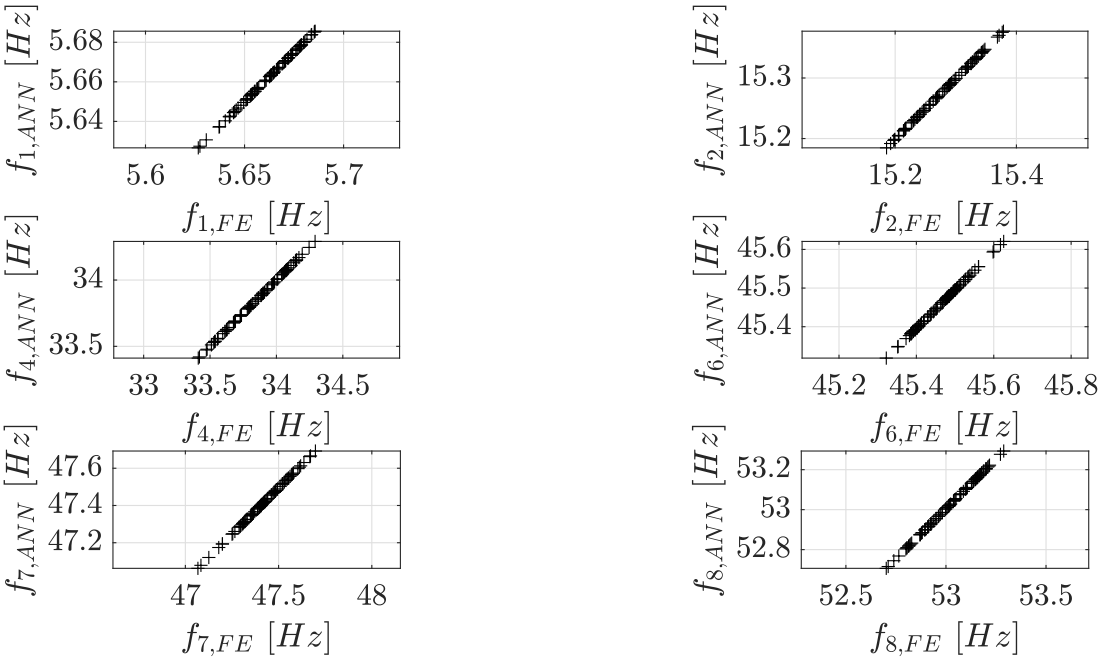

Figure 2: Plot of 100 randomly drawn samples (which are not included in the training set) from the model against the prediction of the ANN for 6 eigenfrequencies in the set.

3.3 Results and discussion

Due to the high dimensionality and general non-convexity of the optimisation problem, introduced in eq. (5), the minimisation is performed using a hybrid optimisation approach. In a first step, a rough estimation fo the global minimum is searched with the Particle Swarm Optimisation algorithm [9]. This estimation of the global optimum is then used as an initial estimate for a sequential quadratic programming approach [12]. Specifically, a swarm size of 250 uncertain model evaluations is used, and the algorithm is deemed to be converged to approximatly the global optimum when it stalls for 10 generations. As a result of using the Particle Swarm algorithm, no initial assumptions on the constituting uncertainty are needed for the identification.

The identification is performed using respecitively $d_r = 7$ and $d_r = 13$ orthogonal base vectors for the reduction of the set of the 26-dimensional measurement data set $\tilde{\mathbf{y}}_m$ and the uncertain realisation set $\tilde{\mathbf{y}}_s$. For both identification procedures, $d_r^+ = 2$, leading to respectively 21 and 78 projections of the d_r dimensional vector space in which $\tilde{\mathbf{y}}_s^r$ is defined. The results of these identification runs are listed in table 3. These results are normalised with respect to the *goal* multivariate interval uncertainty (indicatede with an asteriks in 3).

As can be seen, no identification succeeds in finding the exact parameterset, based on the limited set of measurement data. However, the identification with $d_r = 13$ provides the best results of the two datasets, since more orthogonal base vectors are included herein. A first reason for not obtaining the exact parameters is that not all extreme realisations of the interval

uncertainty at the input of the model are included in the measurement data set, making an exact identification impossible. The root cause however for this, is that the used optimisation algorithms are not capable of finding the exact global minimum of eq. (12) due to the high dimensionality of the search space (28 independent parameters) and the general non-convexity of eq. (12). This inherently leads to inaccuracies in the identification.

Table 3: Parameters that are used in the identification

Parameter	$\underline{\alpha}_1^*$	$\underline{\alpha}_2^*$	$\underline{\alpha}_1 - 7$	$\underline{\alpha}_2 - 7$	$\underline{\alpha}_1 - 13$	$\underline{\alpha}_2 - 13$
γ_1	$1.25 \cdot 10^{02}$	$1.32 \cdot 10^{02}$	0.88	0.9	1.01	0.99
γ_2	$6.30 \cdot 10^{01}$	$7.50 \cdot 10^{01}$	0.01	1.26	0.99	0.99
γ_3	$9.00 \cdot 10^{06}$	$1.30 \cdot 10^{07}$	0.98	1.04	0.98	0.92
γ_4	$1.50 \cdot 10^{09}$	$2.10 \cdot 10^{09}$	0.75	1.05	1	0.98
γ_5	$1.50 \cdot 10^{-01}$	$2.30 \cdot 10^{-01}$	0.98	1.02	1.03	0.99
γ_6	$1.75 \cdot 10^{-01}$	$2.12 \cdot 10^{-01}$	1.01	1.03	0.95	1.02
γ_7	$1.00 \cdot 10^{-02}$	$1.35 \cdot 10^{-02}$	1.05	0.81	0.89	0.93
γ_8	$1.10 \cdot 10^{-02}$	$1.58 \cdot 10^{-02}$	1.05	0.95	0.98	1.11
γ_9	$1.12 \cdot 10^{-02}$	$1.70 \cdot 10^{-02}$	1.05	0.97	1.13	0.98
γ_{10}	$1.85 \cdot 10^{07}$	$2.00 \cdot 10^{07}$	0.99	1.05	1.02	0.99
γ_{11}	$1.95 \cdot 10^{07}$	$2.35 \cdot 10^{07}$	0.98	1.00	1.01	0.99
γ_{12}	$6.35 \cdot 10^{06}$	$7.10 \cdot 10^{06}$	1.00	0.89	0.93	1.20
γ_{13}	$4.45 \cdot 10^{07}$	$5.00 \cdot 10^{07}$	1.00	0.98	1.10	0.98
γ_{14}	$0.75 \cdot 10^{07}$	$1.02 \cdot 10^{07}$	1.05	0.90	0.75	1.21

The result of the identification with $d_r = 13$ are illustrated in figure 3. This figure shows $d_r^+ = 2$-dimensional cross-sections of the convex hull of physical (non-transformed) model responses for the first 5 eigenfrequencies of the model. As may be noted, the convex hull of the model response (in blue) perfectly circumscribes the set of measurement data points (indicated as black crosses), albeit the result is somewhat over-conservative. However, some over-conservatism still is present in the identification, which is due to the fact that the optimiser did not converge to the exact global minimum. The latter is explained by the high dimensionality of the optimisation problem, as 28 uncertain parameters need to be jointly optimised in order to exactly identify the uncertainty in the model.

4 CONCLUSIONS

The interval method has been proven to deliver an accurate, objective representation of the uncertainty that is present in the parameters of a numerical model, even when the datasets on this uncertainty are limited. However, in order to apply these powerfull techniques, a realistic assessment of the uncertainty has to be made, based on measurement data. In this context, the authors presented a novel methodology for the identification and quantification of multivariate interval uncertainty in FE Models [3, 2]. However, the application of this novel methodology to high-dimensional datasets still presents a challenge. This paper therefore introduced a methodology for the reduction of a high-dimensional data set. First, an orthogonal basis is constructed, based on the singular value decomposition of the covariance structure of the measurement data set. This basis is then used to reduce the dimensionality of both the measurement data as the result of the interval FE model. The quantification of the multivariate interval uncertainty, as presented by the authors in [3, 2], is then performed using projections of the datasets on subspaces of this orthogonal basis in order to reduce the computational burden of the analysis.

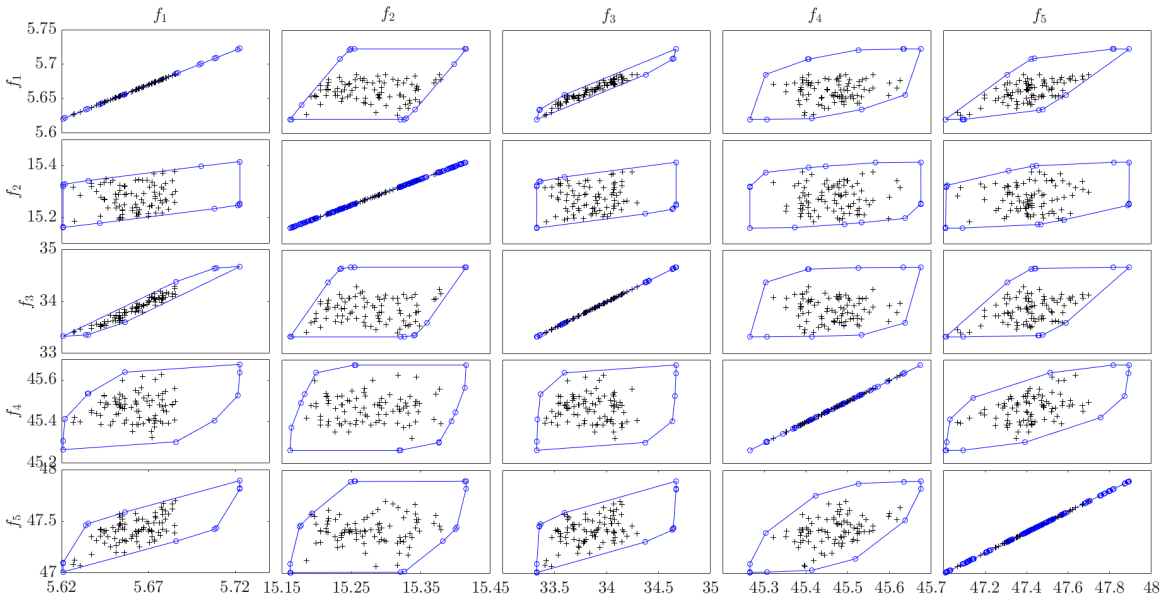

Figure 3: 2-dimensional cross-sections of the convex hull of physical (non-transformed) model responses for the first 5 eigenfrequencies of the model. The response of the identified interval model is indicated in blue, whereas the measurement data points are indicated as black crosses.

The method was illustrated on the AIRMOD test structure, which proved to be a highly challenging example due to the high dimensionality at the input side of the model. As the used optimisation solver failed to converge to the global optimum, over-conservatism was introduced into the identification. Future work will therefore focus on improving this convergence, possibly by applying appropriate scaling and/or using more performing optimisation algorithms. Moreover the identification shall be performed using experimentally obtained modal data.

ACKNOWLEDGEMENTS

The authors would like to gratefully acknowledge dr. Yves Govers from DLR Germany for sharing the Finite Element model of the AIRMOD structure.

REFERENCES

[1] C. Bradford Barber, David P. Dobkin, and Hannu Huhdanpaa. The quickhull algorithm for convex hulls. *ACM Transactions on Mathematical Software*, 22(4):469–483, 1996.

[2] Matthias Faes, Jasper Cerneels, Vandepitte Dirk, and David Moens. Identification and quantification of multivariate interval uncertainty in finite element models. *Computer Methods in Applied Mechanics and Engineering*, 315:896 – 920, 2017.

[3] Matthias Faes, Jasper Cerneels, Dirk Vandepitte, and David Moens. Identification of interval fields for spatial uncertainty representation in finite element models. *Proceedings of the ECCOMAS Congress 2016*, 30:27–30, 2016.

[4] L. Farkas, D. Moens, D. Vandepitte, and W. Desmet. Fuzzy finite element analysis based on reanalysis technique. *Structural Safety*, 32(6):442–448, nov 2010.

[5] Y. Govers, Hh Khodaparast, M. Link, and Je Mottershead. Stochastic Model Updating of the DLR AIRMOD Structure. In *Vulnerability, Uncertainty, and Risk ©ASCE 2014*, number 1974, pages 475–484, Liverpool, 2014.

[6] Y. Govers and M. Link. Stochastic model updatingcovariance matrix adjustment from uncertain experimental modal data. *Mechanical Systems and Signal Processing*, 24(3):696 – 706, 2010.

[7] H Haddad Khodaparast, Y Govers, S Adhikari, M Link, M I Friswell, J E Mottershead, J Sienz, H Haddad Khodaparast, Y Govers, S Adhikari, M Link, M I Friswell, J E Mottershead, J Sienz, and H Haddad Khodaparast. Fuzzy model updating and its application to the DLR AIRMOD test structure. In P Sas, D Moens, and H Denayer, editors, *Proceedings of the International Conference on Uncertainty in Structural Dynamics, USD 2014*, pages 4509–4522, Leuven, Belgium, sep 2014. KU Leuven.

[8] Michael Hanss. The transformation method for the simulation and analysis of systems with uncertain parameters. *Fuzzy Sets and Systems*, 130(3):277–289, sep 2002.

[9] James Kennedy. Particle swarm optimization. In *Encyclopedia of machine learning*, pages 760–766. Springer, 2011.

[10] David J. C. MacKay. Bayesian interpolation. *Neural Comput.*, 4(3):415–447, May 1992.

[11] David Moens and Michael Hanss. Non-probabilistic finite element analysis for parametric uncertainty treatment in applied mechanics: Recent advances. *Finite Elements in Analysis and Design*, 47(1):4–16, 2011.

[12] Jorge Nocedal and Stephen J Wright. *Sequential quadratic programming*. Springer, 2006.

[13] Edoardo Patelli, Yves Govers, Matteo Broggi, Herbert Martins Gomes, Michael Link, and John E. Mottershead. Sensitivity or bayesian model updating: a comparison of techniques using the dlr airmod test data. *Archive of Applied Mechanics*, pages 1–21, 2017.